The FASEB Journal article fj.08-114553. Published online November 21, 2008.

Regulation of the phagocyte NADPH oxidase activity: phosphorylation of gp91^{phox}/NOX2 by protein kinase C enhances its diaphorase activity and binding to Rac2, p67^{phox}, and p47^{phox}

Houssam Raad,* Marie-Hélène Paclet,† Tarek Boussetta,* Yolande Kroviarski,‡ Françoise Morel,† Mark T. Quinn,§ Marie-Anne Gougerot-Pocidalo,*,‡ Pham My-Chan Dang,* and Jamel El-Benna*,[1]

*INSERM, U773, Centre de Recherche Biomédicale Bichat Beaujon CRB3, Université Paris 7 site Bichat, UMRS 773, Paris, France; †GREPI, TIMC-IMAG, UMR CNRS 5525, Centre Hospitalier Universitaire de Grenoble, Grenoble France; ‡AP-HP, Centre Hospitalier Universitaire Xavier Bichat, CIB Phenogen, Paris, France; and §Department of Veterinary Molecular Biology, Montana State University, Bozeman, Montana, USA

ABSTRACT **Neutrophils generate microbicidal oxidants through activation of a multicomponent enzyme called NADPH oxidase. During activation, the cytosolic NADPH oxidase components (p47^{phox}, p67^{phox}, p40^{phox}, and Rac2) translocate to the membranes, where they associate with flavocytochrome b_{558}, which is composed of gp91^{phox}/NOX2 and p22^{phox}, to form the active system. During neutrophil stimulation, p47^{phox}, p67^{phox}, p40^{phox}, and p22^{phox} are phosphorylated; however, the phosphorylation of gp91^{phox}/NOX2 and its potential role have not been defined. In this study, we show that gp91^{phox} is phosphorylated in stimulated neutrophils. The gp91^{phox} phosphoprotein is absent in neutrophils from chronic granulomatous disease patients deficient in gp91^{phox}, which confirms that this phosphoprotein is gp91^{phox}. The protein kinase C inhibitor GF109203X inhibited phorbol 12-myristate 13-acetate–induced phosphorylation of gp91^{phox}, and protein kinase C (PKC) phosphorylated the recombinant gp91^{phox}-cytosolic carboxy-terminal flavoprotein domain. Two-dimensional tryptic peptide mapping analysis showed that PKC phosphorylated the gp91^{phox}-cytosolic tail on the same peptides that were phosphorylated on gp91^{phox} in intact cells. In addition, PKC phosphorylation increased diaphorase activity of the gp91^{phox} flavoprotein cytosolic domain and its binding to Rac2, p67^{phox}, and p47^{phox}. These results demonstrate that gp91^{phox} is phosphorylated in human neutrophils by PKC to enhance its catalytic activity and assembly of the complex. Phosphorylation of gp91^{phox}/NOX2 is a novel mechanism of NADPH oxidase regulation.—Raad, H., Paclet, M.-H., Boussetta, T., Kroviarski, Y., Morel, F., Quinn, M. T., Gougerot-Pocidalo, M.-A., Dang, P. M.-C., El-Benna, J. Regulation of the phagocyte NADPH oxidase activity: phosphorylation of gp91^{phox}/NOX2 by protein kinase C enhances its diaphorase activity and binding to Rac2, p67^{phox}, and p47^{phox}. *FASEB J.* 23, 000–000 (2009)**

Key Words: neutrophils · PMN · cytochrome b558 · inflammation · innate immunity

PROFESSIONAL PHAGOCYTIC CELLS play a central role in defending the host against microorganisms by producing reactive oxygen species (ROS) *via* the NADPH oxidase enzyme complex (1–3). This multicomponent enzyme is dormant in unstimulated cells but can be activated by various stimuli. In the activated form, the NADPH oxidase complex mediates the transfer of electrons from cytosolic NADPH to O_2 to produce the superoxide anion ($O_2^{\cdot -}$) (4). $O_2^{\cdot -}$ is the precursor of other toxic ROS, such as hydrogen peroxide (H_2O_2), the hydroxyl radical ($OH^{\cdot}$), and hypochlorous acid (HOCl), which are involved in bacterial and other microbial destruction (4–6). The NADPH oxidase consists of a membrane-bound flavocytochrome b_{558} and 4 cytosolic subunits: p47^{phox}, p67^{phox}, p40^{phox}, and Rac1/2 (3, 6–10). Activation of the NADPH oxidase is initiated by the assembly of cytosolic factors with flavocytochrome b_{558} to form a complex at the plasma membrane or phagosomal membrane (6–10).

Flavocytochrome b_{558} is the central catalytic core of the oxidase and is a heterodimer composed of 2 integral membrane proteins, p22^{phox} and gp91^{phox} (recently renamed NOX2) (10). The N-terminal domain of gp91^{phox}/NOX2 is hydrophobic, with 6 putative transmembrane helices that likely coordinate 2 heme groups, which are stacked to span the membrane (8, 10). The more hydrophilic C-terminal domain is cytosolic and contains a flavoprotein domain, which is homologous to known flavoprotein dehydrogenase flavin adenine dinucleotide (FAD) binding sequences, as well as a consensus sequence representing a putative NADPH-binding site (10). The acquisition of heme by gp91^{phox}/NOX2 is important for the stability of gp91^{phox}/NOX2 and p22^{phox}, as well as flavocyto-

[1] Correspondence: INSERM U773, CRB3, Faculté de Medecine Xavier Bichat, 16 rue Henri Huchard, 75018 Paris, France. E-mail: jamel.elbenna@inserm.fr

doi: 10.1096/fj.08-114553

chrome b_{558} assembly (11, 12). It is clear that the gp91^{phox}/NOX2 protein alone is the catalytic core of the NADPH oxidase, because it contains all of the required electron transfer cofactors and can produce $O_2^{\cdot -}$ in the absence of other cytosolic components (13–15). Catalysis of $O_2^{\cdot -}$ appears to occur by a 2-step process. In a first catalytic step, the cytosolic C-terminal domain of gp91^{phox}/NOX2 binds NADPH and transfers electrons to the proximal heme *via* its flavin center, whereas the second involves heme transfer of the electron to O_2. Note that the first step catalyzed by the flavin center is called NADPH diaphorase activity (16–19). In addition to serving as the catalytic subunit of the NADPH oxidase, flavocytochrome b_{558} is the central docking component for the cytosolic components p47^{phox}, p67^{phox}, and Rac (7–10).

The importance of NADPH oxidase function in host defense is illustrated by a life-threatening genetic disorder called chronic granulomatous disease (CGD), in which the phagocyte oxidase is dysfunctional, leading to life-threatening bacterial and fungal infections (2, 20). CGD results from mutations in the NADPH oxidase component genes, and the most frequent form of CGD (~65% of all cases) is the X-linked gp91^{phox}-deficient form (X°-CGD) (2, 20).

Several stimuli, such as phorbol myristate acetate (PMA), N-formyl-methionyl-leucyl-phenylalanine (fMLP), and opsonized zymosan (OPZ), can activate the neutrophil NADPH oxidase. NADPH oxidase activation is accompanied by phosphorylation of p47^{phox}, p67^{phox}, p40^{phox}, and p22^{phox} (21–26). Activation requires phosphorylation of p47^{phox} (22) and cotranslocation with p67^{phox} from cytosol to the membrane, followed by association of these proteins with flavocytochrome b_{558} (27–30). In contrast, the phosphorylation of gp91^{phox}/NOX2 and its role in NADPH oxidase activation has not been defined.

In the present study, we clearly show that gp91^{phox}/NOX2 is phosphorylated during activation of human neutrophils, we provide evidence that protein kinase C (PKC) is involved in this process, and we show that phosphorylation potentiates intrinsic diaphorase activity of gp91^{phox}/NOX2 and interaction with Rac, p67^{phox}, and p47^{phox}. These results suggest that phosphorylation of gp91^{phox}/NOX2 by PKC also participates in the regulation of phagocyte NADPH oxidase activity.

MATERIALS AND METHODS

Materials

PMA, fMLP, phenylmethylsulfonylfluoride (PMSF), diisopropyl fluorophosphate (DFP), iodonitrotetrazolium (INT), diphenyleneiodonium (DPI), FAD, and other chemicals were purchased from Sigma Aldrich (St. Louis, MO, USA). Sodium dodecyl sulfate-polyacrylamide gel electrophoresis (SDS-PAGE) and Western blotting reagents were purchased from Bio-Rad (Richmond, CA, USA). PKC and GF109203X were purchased from Calbiochem (San Diego, CA, USA). [γ-^{32}P-ATP], ^{32}P orthophosphoric (H_3PO_4), gamma-bind sepharose beads, pGEX-6p1, and gluthathione sepharose were purchased from GE Healthcare (Little Chalfont, UK).

Monoclonal mouse anti-gp91^{phox} (clone 54.1) and anti-p22^{phox} (clone 44.1) antibodies that recognize specific epitopes localized in the C-terminal intracellular domains of the proteins were described previously (31). Polyclonal rabbit anti-gp91^{phox} and anti-p22^{phox} antibodies raised against polypeptides corresponding to the C-terminal regions of gp91^{phox} (residues 562–569) and p22^{phox} (residues 184-195) were described previously (32). Polyclonal rabbit anti-p47^{phox} and anti-p67^{phox} antibodies were previously described (23, 24). Anti-Rac antibody was from BD Bioscience (Palo Alto, CA, USA).

Neutrophil preparation

Neutrophils were isolated from blood of healthy volunteers by dextran sedimentation and Ficoll centrifugation using phosphate-free buffer [10 mM HEPES, 137 mM NaCl, 5.4 mM KCl, mM $MgCl_2$, 5.6 mM glucose, and 0.025% bovine serum albumin (BSA), pH 7.4], as described previously (33, 34). The isolated cells were resuspended at 10^8 cells/ml in phosphate-free buffer, treated with DFP (2.7 mM) for 20 min at 4°C, and washed in the same buffer.

^{32}P labeling and stimulation

Neutrophils were incubated in phosphate-free buffer containing 0.5 mCi of ^{32}P orthophosphoric acid/10^8 cells/ml for 60 min (33, 34). After centrifugation, the radiolabeled cells were resuspended in the same buffer containing1 mM $CaCl_2$ and incubated at 37°C for 5 min. Following incubation, different stimulatory agents (200 ng/ml PMA, 1 μM fMLP, or 0.5 mg/ml serum OPZ) were added for various lengths of time. The reactions were terminated by adding 10-fold excess of ice-cold phosphate-free loading buffer containing 25 mM NaF and 5 mM EDTA and centrifuged immediately (400 *g* for 12 min at 4°C).

Neutrophil fractionation and immunoprecipitation

The technique used for cell lysis and gp91^{phox} immunoprecipitation was adapted from 2 protocols (35, 36). Cells were lysed by resuspending (5×10^7 cells/ml) in lysis buffer [8 mM HEPES (pH 7.4), 2% Triton X-100, 25 mM NaF, 5.4 mM Na_3VO_4, 2 mM β-glycerophosphate, 1 mM levamisole, 1 mM p-NPP, P8340 protease inhibitor cocktail (1:1000 dilution), 8 mM NaCl, 80 mM KCl, 0.8 mM EDTA, 8 μg/ml chymostatin, 0.8 mM PMSF, 0.08 mM dithiothreitol (DTT), and 1 mM DFP]. After sonication on ice and mixing by rotation, the lysates were centrifuged at 114,000 *g* for 30 min at 4°C. The supernatants were diluted twice in buffer containing 10 mM HEPES, pH 7.4; 10 mM NaCl; 100 mM KCl; 1 mM EDTA; 10 μg/ml chymostatin; and 1 mM PMSF. Immunoprecipitation was performed by addition of anti-gp91^{phox} or anti-p22^{phox} (1/200: dilution) monoclonal antibodies and protein A/G beads (Santa Cruz Biotech, Santa Cruz, CA, USA) saturated in BSA and incubating for 4 h. Beads were then washed 4 times, and proteins were denaturated in Laemmli sample buffer (37) by boiling at 100°C for 3 min.

Deglycosylation of gp91phox/NOX2

Immunoprecipitated gp91^{phox} was denaturated by boiling for 1 min in denaturation buffer, following the protocol supplied by the manufacturer (New England BioLabs, Ipswich, MA, USA). After cooling the tube on ice, reaction buffer contain-

ing 30 mM n-octyl glucoside and N-glycosidase F (PNGase F) (5 U) was added, and the samples were incubated for 2 h at 37°C (38). At the end of incubation an equal volume of 2× Laemmli sample buffer was added to the reaction, followed by boiling for 1 min and analysis by SDS-PAGE, immunoblotting, and autoradiography.

Electrophoresis, immunoblotting, and autoradiography

Immunoprecipitated proteins were separated on SDS-polyacrylamide gels using standard techniques (37). Proteins were transferred to nitrocellulose or polyvinylidene difluoride (PVDF), and phosphorylation of gp91^{phox} was monitored by autoradiography. Gp91^{phox} and p22^{phox} were monitored by immunoblotting, as described previously (33, 34), using anti-gp91^{phox} monoclonal or polyclonal antibodies (1:2000 dilution) and horseradish peroxidase-conjugated anti-mouse or anti-rabbit secondary antibodies.

Measurement of neutrophil ROS production

Luminol-amplified chemiluminescence was measured as described previously (39). Briefly, neutrophil suspensions (5×10^5 cells) in 0.5 ml HBSS containing 10 μM luminol were preheated to 37°C in the luminometer thermostated chamber (Berthold-Biolumat LB937; Berthold Technologies, Wildbad, Germany) and allowed to stabilize. After a baseline reading was established, cells were stimulated with 200 ng/ml PMA, and changes in chemiluminescence were monitored.

Bacterial expression of the cytosolic gp91^{phox}/NOX2 (aa 291-570) domain, p47^{phox}, p67^{phox}, and Rac2

The truncated form of gp91^{phox} (aa 291-570) was obtained by PCR using gp91^{phox} cDNA in Blue-Script as template (40) and the following primers: forward primer (CGC **GGA TCC** TCT CAA CAG AAG GTG GT); reverse primer (CCG **CTC GAG** TTA GAA GTT TTC CTT GTT). PCR products were subcloned into the pGEX-6P1 vector (Pharmacia, Piscataway, NJ, USA) and sequenced to rule out unexpected mutations and to confirm the truncation. For expression, the pGEX-6P1 plasmid containing cDNA encoding glutathione *S*-transferase (GST) -NOX2 (291-570) was transformed into BL21 *Escherichia coli,* and the cells were cultured overnight in 100 ml of LB medium containing ampicillin (100 μg/ml) at 37°C. The overnight culture was then diluted 10-fold and allowed to grow until the optical density at 600 nm reached 0.8. Expression of GST-NOX2 (291-570) was induced with isopropyl-β-D-thiogalactoside (20 μM) and FAD (20 μM) overnight at 16°C. Cells were pelleted by centrifuging at 2500 *g* for 25 min, lysed by sonication in lysis buffer (50 mM NaCl; 5 mM $MgCl_2$; 50 mM Tris-HCl, pH 7.5; 1 mM DTT; 1% Triton X-100; and a mixture of protease inhibitors), and centrifuged at 10,000 *g* for 20 min at 4°C. This protocol gave 50% of soluble GST-NOX2 (291-570) and 50% of nonsoluble GST-NOX2 (291-570). The soluble GST-NOX2 (291-570) was affinity purified by incubation of the supernatant with glutathione-Sepharose 4B beads overnight at 4°C. Beads were then washed in lysis buffer, and the fusion protein was eluted with 15 mM glutathione; 50 mM Tris-HCl, pH 8; and 20 μM FAD. To separate NOX2 (291-570) from GST, the recombinant protein was treated with PreScission protease for 6 h at 4°C in 150 mM NaCl; 50 mM Tris-HCl, pH 7; 1 mM DTT; 1 mM EDTA; and 20 μM FAD and subjected to another round of glutathione-bead adsorption. NOX2 (291-570) migrates at 31 kDa as a monomeric protein in a nondenaturating gel (data not shown). P47^{phox}, p67^{phox}, and Rac2 were expressed at 37°C, using the same protocol (pGEX plasmids were a gift from the late B. M. Babior and U. Knaus, Scripps Research Institute, La Jolla, CA, USA).

In vitro phosphorylation of NOX2 (291-570)-domain and p47^{phox}

Phosphorylation by PKC was performed as described previously (41). Briefly, the reaction mixture contained 1 μg of recombinant protein, 25 ng of PKC in 40 mM HEPES, 10 mM $MgCl_2$, 1 mM DTT, 5 μg/ml diacylglycerol, 150 μg/ml phosphatidylserine, 3 mM $CaCl_2$, and 50 μM ATP (containing 1 μCi [γ-^{32}P]-ATP) in a total volume of 50 μl. The reaction was incubated for 30 min at 30°C and terminated by addition of 1 μM staurosporin. In some experiments, proteins were denaturated in Laemmli sample buffer (37) with boiling at 100°C for 3 min.

Phosphoamino acid analysis

Phosphorylated NOX2 (291-570) was separated by SDS-PAGE, transferred to PVDF, excised, and then subjected to hydrolysis with 6 N HCl for 90 min at 110°C (24). The supernatant was dried in a speed-vac and lyophilized. Phosphoamino acids were collected and mixed with or without 2 μg of standard markers (phosphoserine, phosphothreonine, phosphotyrosine) and separated by thin-layer chromatography. Samples were then applied to a cellulose plate and separated by electrophoresis at 1100 V for 45 min at 4°C in a buffer consisting of water/acetic acid/pyridine (189:10:1), pH 3.5. Standard phosphoamino acids were visualized by spraying with 0.2% ninhydrin, and phosphorylated amino acids were detected by autoradiography.

Two-dimensional tryptic phosphopeptide mapping

The nitrocellulose area containing ^{32}P-labeled gp91^{phox}/NOX2 was incubated for 30 min at 37°C with polyvinylpyrrolidone and incubated overnight with trypsin (50 μg/ml) in carbonate buffer. Released peptides were washed 3 times, redissolved in electrophoresis buffer, and applied to one corner of a cellulose thin-layer plate. After electrophoresis (1000 V for 20 min), ascending chromatography was performed in isobutyric acid buffer (21, 23). The plates were autoradiographed at −75°C.

CNBr cleavage of the phosphorylated NOX2 (291-570) domain

Phosphorylated NOX2 (291-570) was separated by SDS-PAGE, transferred to nitrocellulose, excised, and then incubated with 50 mg/ml CNBr in 70% (v/v) formic acid for 16 h at room temperature in the dark. The supernatant was dried in a speed-vac and lyophilized. The peptides were analyzed by Tris-Tricine SDS-PAGE followed by autoradiography (21).

GST pull-down assay

The assay was performed as described by Dang *et al.* (30). Here 80 pmol of GST-Rac2, GST-p67^{phox}, phosphorylated GST-p47^{phox}, and GST alone were incubated in the presence of 5 pmol of phosphorylated or not phosphorylated recombinant NOX2 (291-570) and glutathione-Sepharose beads in interaction buffer (20 mM Hepes, pH 7.5; 1% Nonidet P-40; 50 mM NaCl; and 1 mM EGTA) for 1 h. After washing, the complex was eluted with 10 mM glutathione and analyzed by SDS-PAGE and Western blots using protein-specific antibodies.

Diaphorase activity assay

INT-reductase activity was measured according to the protocols of Han *et al.* (18) and Nisimoto *et al.* (19). The NOX2 (291-570) flavoprotein domain was preincubated with 20 μM FAD for 16 h at 4°C. Activity was measured in 500 μl of assay buffer (0.3% Triton X-100, 50 mM NaCl, 4 mM $MgCl_2$, and 20 μM FAD in 50 mM phosphate buffer, pH 7.3) containing 0.2 mM INT and 1 μg of phosphorylated or unphosphorylated NOX2 (291-570) in the absence or presence of phosphorylated $p47^{phox}$, $p67^{phox}$, and Rac2. The reactions were started by addition of 0.2 mM NADPH at 37°C, and absorbance at 500 nm was monitored. The reaction was performed with or without DPI (20 μM) to check the specificity. The rate of INT reduction was quantified using an extinction coefficient of 11 mM^{-1} cm^{-1}. After addition of NADPH, the INT reductase activity was measured for 6 min, as the absorbance change at 500 nm was almost linear throughout this interval.

Statistical analysis

All results are expressed as means ± SE. Significant differences were identified using a Student's *t* test.

RESULTS

$Gp91^{phox}$/NOX2 is phosphorylated in activated human neutrophils

To evaluate phosphorylation of $gp91^{phox}$/NOX2 in human neutrophils, cells were labeled with ^{32}P and stimulated with PMA. $Gp91^{phox}$/NOX2 was immunoprecipitated from lysates using a specific monoclonal antibody, and the samples were analyzed by SDS-PAGE, immunoblotting, and autoradiography. Our results show that, although $gp91^{phox}$/NOX2 was weakly phosphorylated in resting cells, its phosphorylation was clearly induced in PMA-activated neutrophils (**Fig. 1**, IP anti-NOX2). Furthermore, corresponding Western blot analysis identified this phosphoprotein as $gp91^{phox}$/NOX2 and showed that the same amount of protein was present for each condition. $Gp91^{phox}$/NOX2 is heavily glycosylated, and its mature form migrates as a broad band in SDS-PAGE with an average size of 91 kDa because of variable glycosylation (42, 43). This broad band in SDS-PAGE is a characteristic signature of $gp91^{phox}$/NOX2. Likewise, the phosphorylated protein and corresponding blot both demonstrate a similar broad band (Fig. 1), which supports the conclusion that the phosphorylated protein corresponds to $gp91^{phox}$/NOX2.

$Gp91^{phox}$/NOX2 and $p22^{phox}$ form a stable heterodimer that can be immunoprecipitated. To further confirm that $gp91^{phox}$ is phosphorylated in human neutrophils, immunoprecipitation was performed with anti-$p22^{phox}$ monoclonal antibody. As shown in Fig. 1 (IP anti-p22phox), phosphorylated $gp91^{phox}$/NOX2 coimmunoprecipitated with $p22^{phox}$, and the corresponding Western blot analysis showed that the same amount of each protein ($gp91^{phox}$/NOX2 and p22phox) was present for each condition. Immunoprecipitation with either anti-$gp91^{phox}$ or anti-$p22^{phox}$ antibodies demonstrated that coprecipitated $p22^{phox}$ was also phosphorylated (Fig. 1), which confirms previous studies by Regier *et al.* (26). An important fact is that corresponding Western blot analysis showed that the same amount of proteins is present for each condition (Fig. 1), whereas immunoprecipitation with control IgG showed no phosphorylated proteins in the gel (data not shown). Thus, in the following experiments reported here, phosphorylation of $gp91^{phox}$ was confirmed by immunoprecipitation with both antibodies.

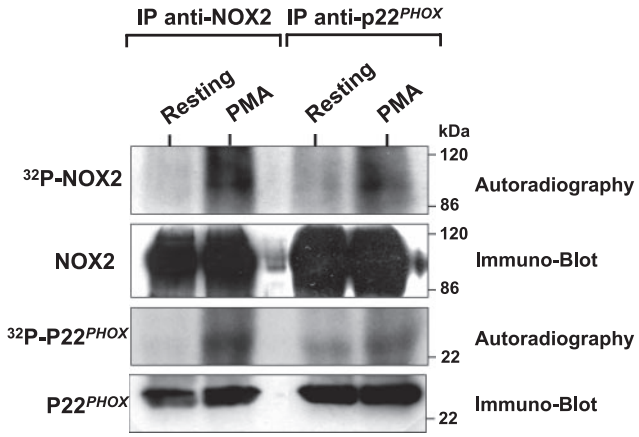

Figure 1. Analysis of $gp91^{phox}$/NOX2 phosphorylation in PMA-activated human neutrophils. ^{32}Pi-labeled neutrophils (5×10^7 cells/ml) were incubated in the absence (resting) or presence of PMA (200 ng/ml for 8 min). Cell lysates were prepared and immunoprecipitated with monoclonal anti-$gp91^{phox}$ (IP anti-NOX2) and anti-$p22^{phox}$ (IP anti-$p22^{phox}$) antibodies, as described in Materials and Methods. Proteins were subjected to SDS-PAGE, blotted on nitrocellulose, and detected by autoradiography (^{32}P-NOX2) and immunoblotting with anti-$gp91^{phox}$ (NOX2) and anti-$p22^{phox}$ antibodies ($p22^{phox}$). Data are representative of 4 experiments.

To further establish that the phosphorylated broad band corresponds to $gp91^{phox}$/NOX2, we utilized 2 additional approaches. First, we performed the same experiment as described in Fig. 1 using neutrophils from a CGD patient who has a stop mutation in *CYBB,* the gene encoding $gp91^{phox}$/NOX2. This mutation results in a complete deficiency in $gp91^{phox}$ expression (X°-CGD), which we confirmed by immunoblotting (**Fig. 2*A***). In addition, $p22^{phox}$ expression is also absent (Fig. 2*A*), because its expression requires the presence of $gp91^{phox}$/NOX2 (2, 20). Analysis of these cells using the same methods used above to demonstrate $gp91^{phox}$/NOX2 phosphorylation showed that the phosphorylated protein corresponding to ^{32}P-labeled gp91phox/NOX2 was missing in these cells, as compared to control neutrophils isolated from healthy donors (Fig. 2*B*). These data further verify that gp91phox/NOX2 is phosphorylated in activated neutrophils.

Expression of the cytosolic NADPH oxidase components $p47^{phox}$ and $p67^{phox}$ is normal in X°-CGD neutrophils, which was confirmed by immunoblot analysis of CGD and control neutrophil lysates (Fig. 2*A*). Likewise, we show that $p47^{phox}$ is clearly phosphorylated in the same sample preparations (Fig. 2*C*), which indicates that PMA was able to induce cytosolic oxidase protein phosphorylation in X°-CGD neutrophils.

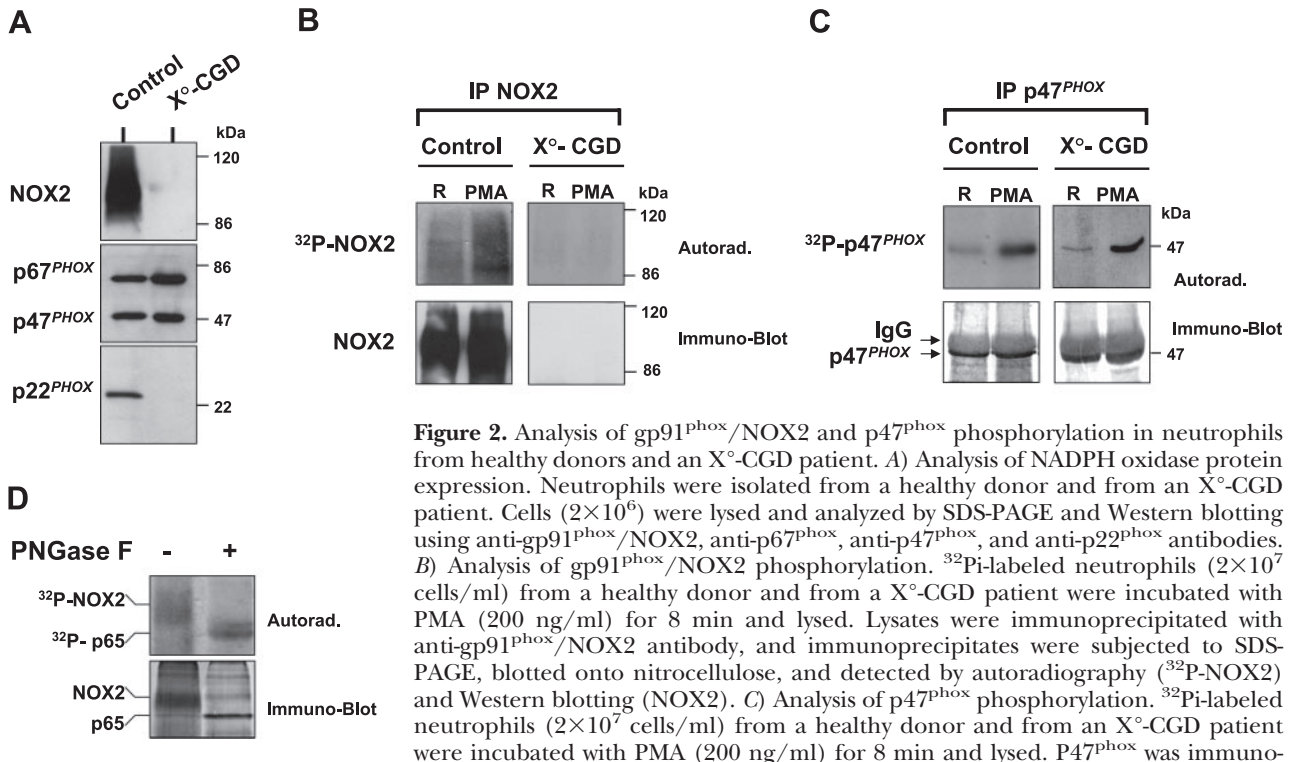

Figure 2. Analysis of gp91^{phox}/NOX2 and p47^{phox} phosphorylation in neutrophils from healthy donors and an X°-CGD patient. *A*) Analysis of NADPH oxidase protein expression. Neutrophils were isolated from a healthy donor and from an X°-CGD patient. Cells (2×10^6) were lysed and analyzed by SDS-PAGE and Western blotting using anti-gp91^{phox}/NOX2, anti-p67^{phox}, anti-p47^{phox}, and anti-p22^{phox} antibodies. *B*) Analysis of gp91^{phox}/NOX2 phosphorylation. ^{32}Pi-labeled neutrophils (2×10^7 cells/ml) from a healthy donor and from a X°-CGD patient were incubated with PMA (200 ng/ml) for 8 min and lysed. Lysates were immunoprecipitated with anti-gp91^{phox}/NOX2 antibody, and immunoprecipitates were subjected to SDS-PAGE, blotted onto nitrocellulose, and detected by autoradiography (^{32}P-NOX2) and Western blotting (NOX2). *C*) Analysis of p47^{phox} phosphorylation. ^{32}Pi-labeled neutrophils (2×10^7 cells/ml) from a healthy donor and from an X°-CGD patient were incubated with PMA (200 ng/ml) for 8 min and lysed. P47^{phox} was immunoprecipitated, analyzed by SDS-PAGE, blotted onto nitrocellulose, and detected by autoradiography (^{32}P-p47^{phox}) and Western blotting (p47^{phox}). *D*) Analysis of deglycosylated gp91^{phox}/NOX2. ^{32}Pi-labeled neutrophils (5×10^7 cells/ml) were incubated with PMA (200 ng/ml) for 8 min and lysed. Lysates were immunoprecipitated with anti-gp91^{phox}/NOX2 antibody, and immunopreciptates were subjected to deglycosylation, as described. Control and deglycosylated samples were subjected to SDS-PAGE, blotted onto nitrocellulose, and detected by autoradiography (^{32}P-NOX2) and Western blotting (NOX2). Data are representative of 3 experiments.

Gp91^{phox}/NOX2 is heavily glycosylated (30% of the molecular mass) and migrates on SDS-PAGE as a broad band, whereas enzymatically deglycosylated protein migrates as a more focused band. Analysis of immunoprecipitated gp91^{phox}/NOX2 after deglycosylation showed that deglycosylated gp91^{phox}/NOX2 runs as sharper band at ~60 kDa (Fig. 2*D*), which confirms previous reports (42). Important to note is that the phosphorylated broad band was also shifted to a sharper, more focused, phosphorylated 60-kDa band, again verifying that the phosphorylated band is indeed gp91^{phox}/NOX2.

Together, we used 3 complementary approaches to demonstrate clearly that the phosphorylated protein immunoprecipitated with the anti-gp91^{phox} antibody used for this study is indeed gp91^{phox}/NOX2 and that gp91^{phox}/NOX2 is phosphorylated during neutrophil activation.

Gp91^{phox}/NOX2 phosphorylation is induced by various agonists

To determine whether gp91^{phox}/ NOX2 phosphorylation was a common feature characteristic of neutrophil activation, we evaluated the ability of various agonists, which are known to activate the NADPH oxidase, to induce gp91^{phox}/NOX2 phosphorylation. As shown in **Fig. 3**, treatment of ^{32}P-labeled neutrophils with PMA, fMLP, and OPZ induced gp91^{phox}/NOX2 phosphorylation, although with differing degrees of potency. As a control, we showed by Western blot analysis that the same amount of gp91^{phox}/NOX2 was immunoprecipitated from each sample. Overall, the relative potency of these agents to induce gp91^{phox}/NOX2 phosphorylation was PMA $\gg$ OPZ $>$ fMLP. Additionally, different concentrations of these agents and various incubation times yielded the same results (not shown).

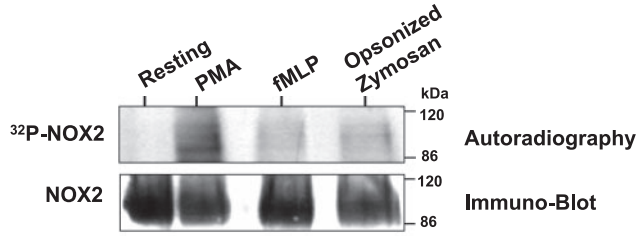

Figure 3. PMA, fMLP, and OPZ induce gp91^{phox}/NOX2 phosphorylation in human neutrophils. ^{32}Pi-labeled neutrophils were incubated with PMA (200 ng/ml for 8 min), fMLP (1×10^{-6} M for 1 min), and OPZ (0.5 mg/ml for 10 min), as indicated. Cells were lysed, and gp91^{phox}/NOX2 was immunoprecipitated, as described. Proteins were separated by SDS-PAGE and analyzed by autoradiography (^{32}P-NOX2) and Western blotting (NOX2). Data are representative of 3 experiments.

Gp91^{phox}/NOX2 phosphorylation parallels NADPH oxidase activation and is inhibited by the PKC inhibitor GF109203X

To study the kinetics of gp91^{phox}/NOX2 phosphorylation in neutrophils, cells were treated with PMA for 0, 3, 6, and 9 min before lysis and immunoprecipitation. As shown in **Fig. 4*A***, increased gp91^{phox}/NOX2 phosphorylation was detected after 3 min and increased gradually to 9 min after PMA addition. Note that similar levels of gp91^{phox}/NOX2 were present in each lane, as determined by Western blotting (Fig. 4*A*, bottom blots). We also compared the kinetics of gp91^{phox}/NOX2 phosphorylation to the kinetics of ROS production and found that PMA-induced gp91^{phox}/NOX2 phosphorylation directly correlated with the kinetics of ROS production (Fig. 4*B*).

Because the degree of PMA-induced gp91^{phox}/NOX2 phosphorylation was more intense than that induced by other stimuli and PMA is a direct PKC activator, we evaluated whether this kinase played a role in gp91^{phox}/NOX2 phosphorylation. To investigate this possibility, we evaluated the effect of GF109203X, a selective PKC inhibitor on gp91^{phox}/NOX2 phosphorylation in PMA stimulated human neutrophils. As shown in Fig. 4*C*, GF109203X dose-dependently inhibited gp91^{phox}/NOX2 phosphorylation in PMA-treated neutrophils. Treatment with GF109203X also inhibited fMLP-induced gp91^{phox}/NOX2 phosphorylation and neutrophil $O_2^{\cdot-}$ production (data not shown).

The gp91^{phox}/NOX2 cytosolic flavoprotein domain is phosphorylated by PKC *in vitro* and in PMA-stimulated neutrophils

The results reported above strongly suggest that PKC is involved in gp91^{phox}/NOX2 phosphorylation in human neutrophils. To determine whether PKC can directly phosphorylate gp91^{phox}/NOX2, we first analyzed gp91^{phox}/NOX2 cytosolic sequences for potential PKC-phosphorylation sites using the NetPhos 2.0 Server and protein Scan program for PKC sites (NCI, Bethesda, MD, USA). Gp91^{phox}/NOX2 is an integral membrane protein that is predicted to have a cytosolic N terminus, 2 cytosolic intracellular loops, and a cytosolic C terminus containing a flavoprotein domain (8, 10). Scanning these cytosolic regions for potential phosphorylation sites indicated none in the N-terminal sequence and only 2 in the cytosolic loops. In contrast, the cytosolic flavoprotein domain has up to 8 potential phosphorylation sites. Thus, we evaluated whether PKC could phosphorylate the gp91^{phox}/NOX2 cytosolic flavoprotein domain [NOX2 (291-570)]. As shown in **Fig. 5**, purified recombinant GST-NOX2 (291-570) fusion protein (Fig. 5*A*) was phosphorylated *in vitro* by PKC in a time-dependent manner (Fig. 5*B*), whereas control GST alone was not phosphorylated by PKC (data not shown). Likewise, PKC was also able to phosphorylate native gp91^{phox} immunoprecipitated from resting neutrophils (data not shown). Furthermore, phosphoamino acid analysis of PKC-phosphorylated NOX2 (291-570) showed that this protein was phosphorylated on serine and threonine residues (Fig. 5*C*), supporting a role for PKC-mediated phosphorylation. To further

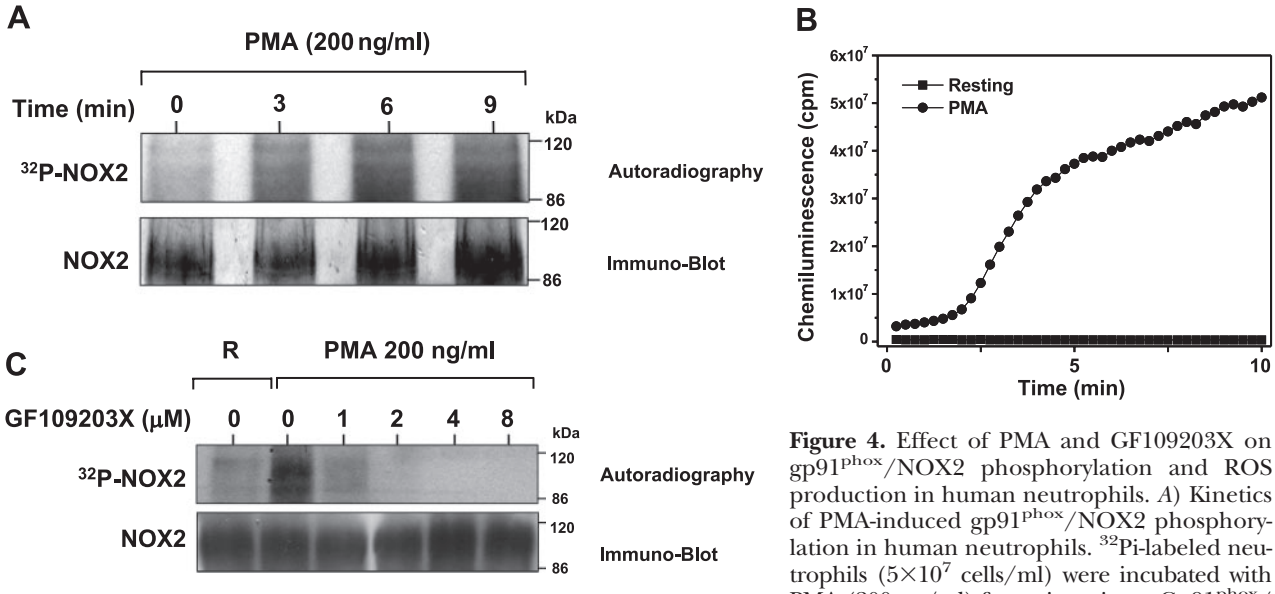

Figure 4. Effect of PMA and GF109203X on gp91^{phox}/NOX2 phosphorylation and ROS production in human neutrophils. *A*) Kinetics of PMA-induced gp91^{phox}/NOX2 phosphorylation in human neutrophils. ^{32}Pi-labeled neutrophils (5×10^7 cells/ml) were incubated with PMA (200 ng/ml) for various times. Gp91^{phox}/NOX2 was immunoprecipitated, and samples were subjected to SDS-PAGE, blotted on nitrocellulose, and detected by autoradiography (^{32}P-NOX2) and Western blotting (NOX2). *B*) Kinetics of PMA-induced NADPH oxidase activation in human neutrophils. Human neutrophils (5×10^5 cells/0.5 ml Hank's buffer) were treated with buffer or PMA (200 ng/ml), and luminol-amplified chemiluminescence was measured. *C*) Effect of the PKC inhibitor GF109203X on gp91^{phox}/NOX2 phosphorylation in human neutrophils. ^{32}Pi-labeled neutrophils were incubated in the presence or absence of GF109203X (1–8 μM) for 15 min, stimulated with PMA (200 ng/ml) for 8 min, and gp91^{phox}/NOX2 was immunoprecipitated from lysates. Lysates were analyzed by autoradiography (^{32}P-NOX2) and immunoblotting (NOX2). Data are representative of 3 experiments.

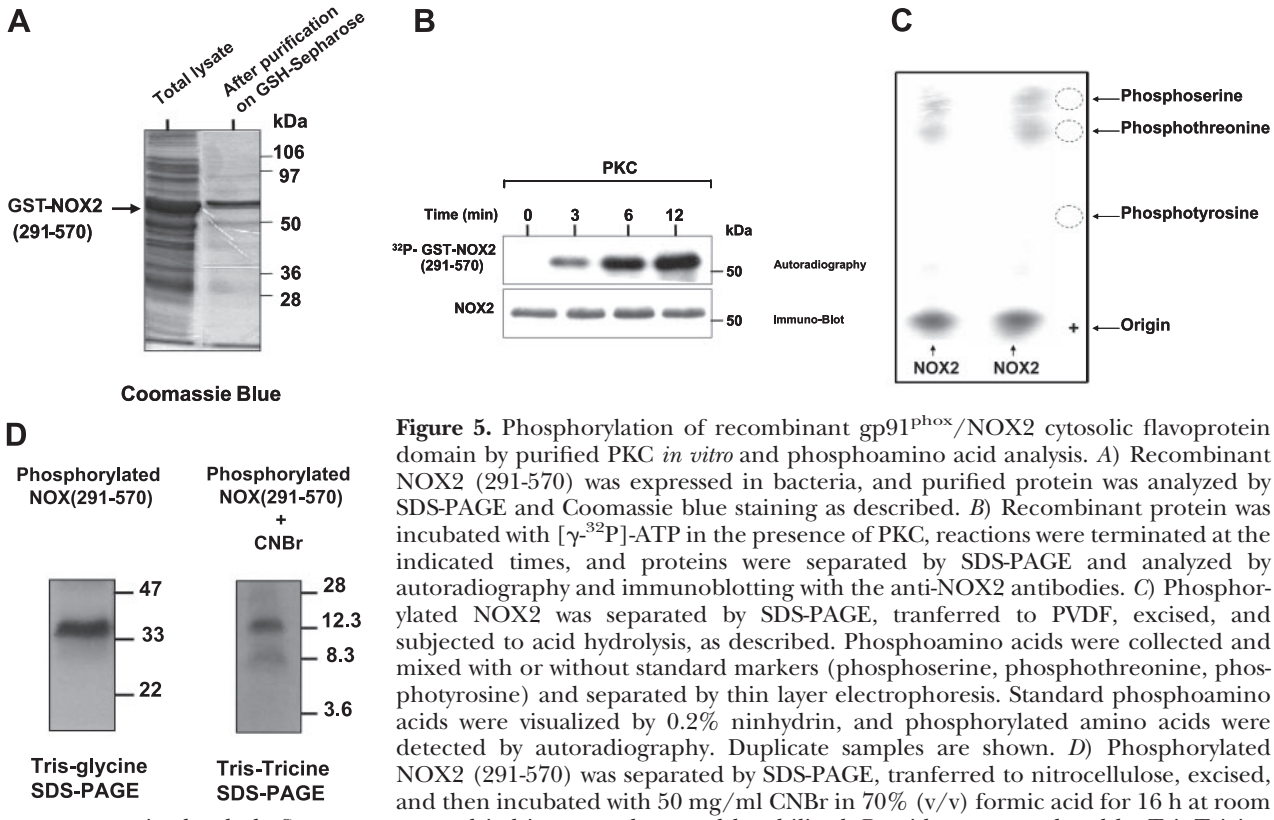

Figure 5. Phosphorylation of recombinant gp91^{phox}/NOX2 cytosolic flavoprotein domain by purified PKC *in vitro* and phosphoamino acid analysis. *A*) Recombinant NOX2 (291-570) was expressed in bacteria, and purified protein was analyzed by SDS-PAGE and Coomassie blue staining as described. *B*) Recombinant protein was incubated with [γ-^{32}P]-ATP in the presence of PKC, reactions were terminated at the indicated times, and proteins were separated by SDS-PAGE and analyzed by autoradiography and immunoblotting with the anti-NOX2 antibodies. *C*) Phosphorylated NOX2 was separated by SDS-PAGE, tranferred to PVDF, excised, and subjected to acid hydrolysis, as described. Phosphoamino acids were collected and mixed with or without standard markers (phosphoserine, phosphothreonine, phosphotyrosine) and separated by thin layer electrophoresis. Standard phosphoamino acids were visualized by 0.2% ninhydrin, and phosphorylated amino acids were detected by autoradiography. Duplicate samples are shown. *D*) Phosphorylated NOX2 (291-570) was separated by SDS-PAGE, tranferred to nitrocellulose, excised, and then incubated with 50 mg/ml CNBr in 70% (v/v) formic acid for 16 h at room temperature in the dark. Supernatant was dried in a speed-vac and lyophilized. Peptides were analyzed by Tris-Tricine SDS-PAGE followed by autoradiography. Data are representative of 4 experiments.

map the region of NOX2 (291-570) that contains the phosphorylated residues, the protein was cleaved by CNBr, which cleaves the proteins on methionine residues, and the peptides were analyzed by Tris-Tricine SDS-PAGE followed by autoradiography. The predicted peptides by CNBr cleavage of the (291-570) domain are aa 291-312 (molecular mass 2.5 kDa), 313-320 (1 kDa), 321-405 (10 kDa), 406-465 (7 kDa), and 466-570 (13 kDa). The phosphorylated NOX2 (291-570) domain migrated as expected at 34 kDa. Treatment of this protein with CNBr followed by Tris-Tricine gel electrophoresis produced 2 phosphorylated fragments of 13 and 10 kDa (Fig. 5*D*). These results show that gp91phox/NOX2 is phosphorylated in its carboxy-terminal fragment on sites located in the 2 sequences aa 321-405 and 466-570.

To determine whether phosphorylation of the gp91^{phox}/NOX2-cytosolic tail *in vitro* and the phosphorylation of gp91^{phox}/NOX2 in intact neutrophils occurred on the same or on different peptides, we analyzed phosphorylated proteins by 2-dimensional tryptic phosphopeptide mapping of these samples. These analyses showed that gp91^{phox}/NOX2 in PMA-stimulated neutrophils is phosphorylated on several peptides, designated as peptides a, b, and c (**Fig. 6**), and the relative level of phosphorylation intensity in

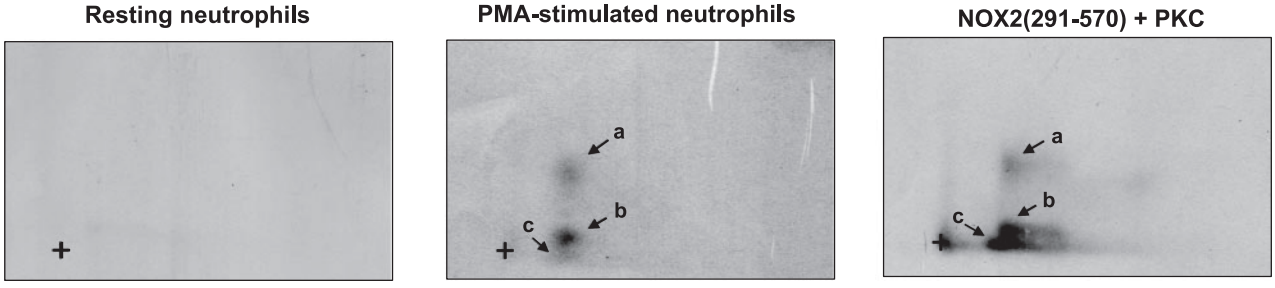

Figure 6. Tryptic phosphopeptide mapping of phosphorylated gp91^{phox}/NOX2 isolated from PMA-activated neutrophils and recombinant gp91^{phox}/NOX2 (291-570) phosphorylated *in vitro* by PKC. ^{32}Pi-labeled neutrophils were incubated with or without PMA (200 ng/ml) for 8 min, and gp91^{phox}/NOX2 was immunoprecipitated. Recombinant NOX2 (291-570) was incubated with [γ-^{32}P]-ATP in the presence of PKC, reactions were terminated at the indicated times, and proteins were separated by SDS-PAGE and analyzed by autoradiography. ^{32}P-gp91^{phox}/NOX2 and ^{32}P- NOX2 (291-570) were recovered from nitrocellulose sheets and submitted to trypsin digestion. Peptides were subjected to first-dimension electrophoresis and second-dimension liquid chromatography, as described. Phosphorylated peptides were detected by autoradiography. Data are representative of 3 experiments.

these peptides was b > a ≫ c. Phosphopeptide mapping analysis of the recombinant gp91^{phox}/NOX2-cytosolic tail phosphorylated *in vitro* by PKC showed that the same peptides (a, b, and c) were phosphorylated, although with different relative intensities than in intact neutrophils (Fig. 6). These results suggest that PKC phosphorylates the same gp91^{phox}/NOX2 sites in intact cells and *in vitro,* and that these sites are located in the carboxy-terminal region of the protein.

Phosphorylation of the gp91^{phox}/NOX2 cytosolic flavoprotein domain stimulates its interaction with Rac2, p67^{phox}, and p47^{phox}

Gp91^{phox}/NOX2 was shown to interact with the cytosolic components Rac2, p67^{phox}, and p47^{phox} (30, 44). Thus, we studied the consequences of PKC-mediated phosphorylation of recombinant NOX2 (291-570) on these interactions. Results showed (**Fig. 7**) that nonphosphorylated NOX2 (291-570) is able to interact with Rac2, p67^{phox}, and phosphorylated p47^{phox}, which is consistent with previous reports (30, 44). Interestingly, phosphorylation of NOX2 (291-570) by PKC induced a clear increase in these interactions, which suggests that phosphorylation of gp91^{phox}/NOX2 may potentiate the assembly of NADPH oxidase. Control experiments with GST alone showed no interaction with NOX2.

Phosphorylation of the gp91^{phox}/NOX2 cytosolic flavoprotein domain stimulates its diaphorase activity

Gp91^{phox}/NOX2 was shown to have an intrinsic INT-reductase activity, which is also known as diaphorase activity (16–19), and the cytosolic flavoprotein domain (aa 291-570) was shown to be responsible for this activity (18, 19). Thus, we studied the consequences of PKC-mediated phosphorylation of this domain on its intrinsic enzymatic diaphorase activity in the absence or presence of the cytosolic components. In the presence of FAD and NADPH, recombinant NOX2 (291-570) alone has a spontaneous DPI-inhibitable diaphorase activity (**Fig. 8*A***), which is consistent with previous reports (18, 19). It is interesting that phosphorylation of NOX2 (291-570) by PKC induced an increase in DPI-inhibitable diaphorase activity (from 1.13±0.20 μmol reduced-INT/mg protein in the absence of PKC *vs.* 2.74±0.5 μmol reduced-INT/mg protein in the presence of PKC), which corresponds to a 141% increase in activity.

In the presence of Rac2, p67^{phox}, and phosphorylated p47^{phox} (Fig. 8*B*), diaphorase activity of nonphosphorylated NOX2 is higher than NOX2 alone. Phosphorylation of NOX2 (291-570) by PKC and addition of Rac2, p67^{phox}, and phosphorylated p47^{phox} further induced an increase in DPI-inhibitable diaphorase activity (from 2.51±0.13 μmol reduced-INT/mg protein in the absence of PKC *vs.* 4.77±0.31 μmol reduced-INT/mg protein in the presence of PKC), which corresponds to a 90% increase in activity. Taken together, these results suggest that phosphorylation of gp91^{phox}/NOX2 may regulate its catalytic activity in the absence and presence of cytosolic components.

DISCUSSION

In the present study we have demonstrated with several complementary approaches that gp91^{phox}/NOX2 is phosphorylated in human neutrophils by several agents known to induce NADPH oxidase activation, such as PMA, fMLP, and OPZ. In addition, we provide evidence that this phosphorylation is mediated by PKC, which is able to directly phosphorylate gp91^{phox}/NOX2 *in vitro,* resulting in a stimulation of the interaction with p47^{phox}, p67^{phox}, and Rac2, and enhanced diaphorase activity by this domain. Here we demonstrate that phosphorylation of gp91phox/NOX2 itself is a novel mechanism of regulation of NADPH oxidase activity in addition to the other known mechanisms.

Gp91^{phox}/NOX2 is heavily glycosylated, and its mature form migrates as a broad band in SDS-PAGE, which is due to variable glycosylation (42, 43). This

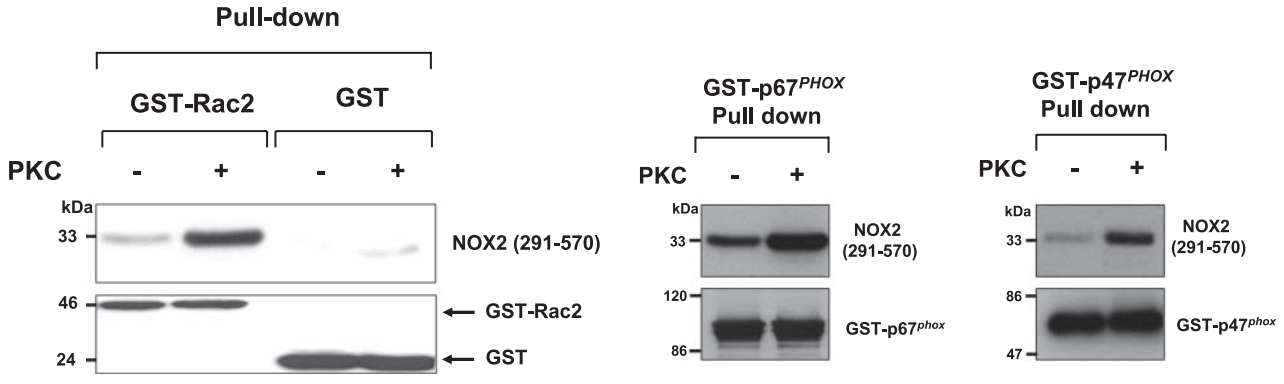

Figure 7. Effect of PKC-induced phosphorylation of gp91^{phox}/NOX2-cytosolic flavoprotein domain on interaction with p47^{phox}, p67^{phox}, and Rac2. GST-Rac2, GST-p67^{phox}, phosphorylated GST-p47^{phox}, and GST alone were incubated in the presence of 5 pmol of phosphorylated or nonphosphorylated recombinant NOX2 (291-570) and glutathione-Sepharose beads in interaction buffer for 1 h. After washing, the complex was eluted with reduced glutathione and analyzed by SDS-PAGE and Western-Blots using protein specific antibodies. Data are representative of 3 experiments.

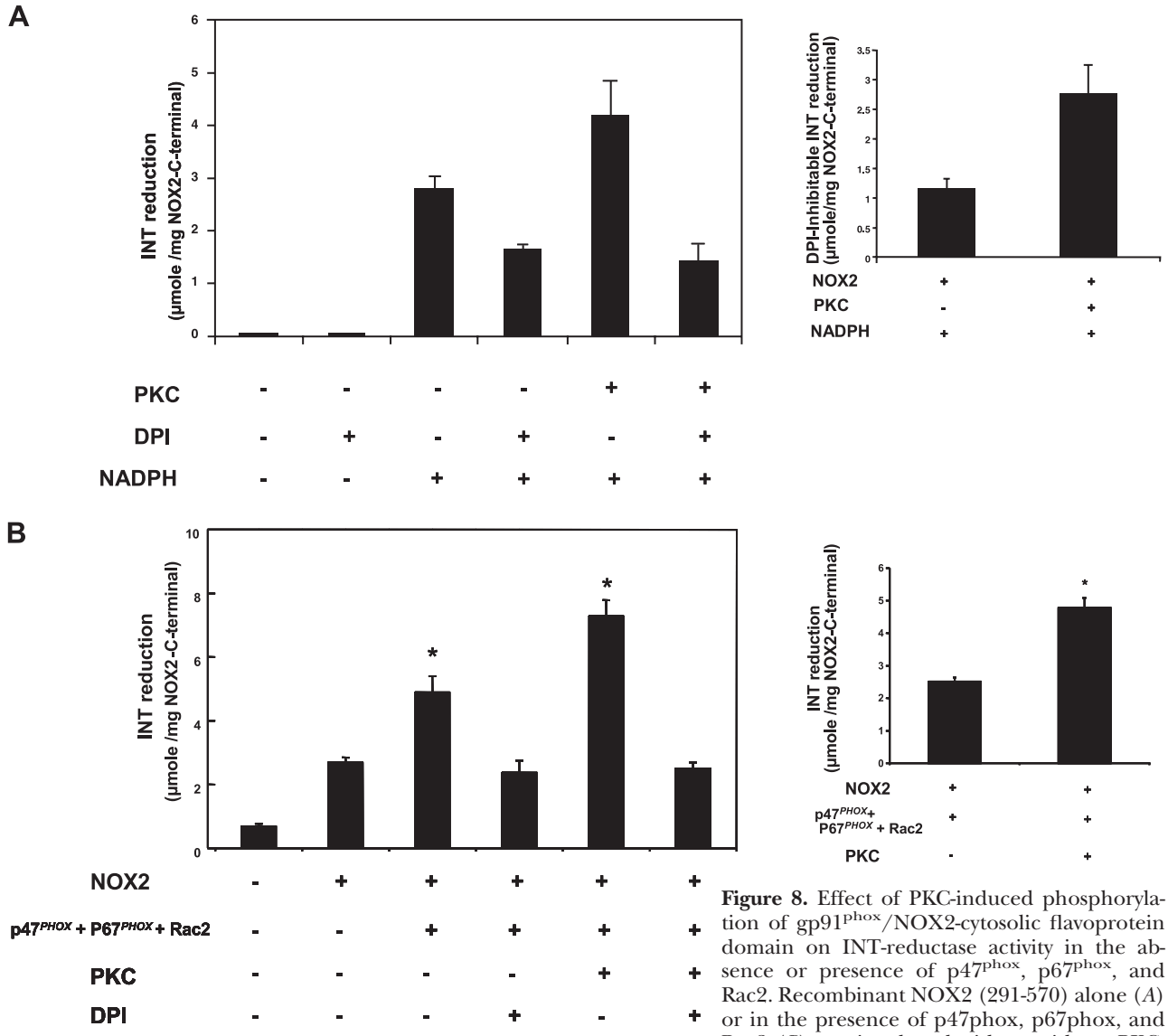

Figure 8. Effect of PKC-induced phosphorylation of gp91^{phox}/NOX2-cytosolic flavoprotein domain on INT-reductase activity in the absence or presence of p47^{phox}, p67^{phox}, and Rac2. Recombinant NOX2 (291-570) alone (*A*) or in the presence of p47phox, p67phox, and Rac2 (*B*) was incubated with or without PKC, and INT-reductase activity was measured. Activity was determined in a 500 µl volume of assay buffer containing 0.2 mM INT and 1 µg of the phosphorylated or nonphosphorylated NOX2 (291-570), which was preincubated with (+) or without (−) DPI (20 µM) for 15 min. Reaction was initiated by addition of 0.2 mM NADPH, and rate of INT reduction was monitored by measuring absorbance at 500 nm. Inserts: DPI-inhibitable INT-reductase activity. Data are representative of 6 experiments. $*P < 0.05$.

broad band is characteristic of gp91^{phox}/NOX2 and constitutes a "signature" of this glycosylated protein. We showed that the phosphorylated protein migrated as a broad band in both the autoradiograph and corresponding blot, indicating that the phosphorylated protein corresponds to gp91^{phox}/NOX2. To further confirm that the phosphorylated band corresponds to gp91^{phox}/NOX2, we performed similar phosphorylation experiments using neutrophils from a gp91^{phox}/NOX2–deficient CGD patient. These studies clearly show that the phosphorylated broad band is missing in gp91^{phox}/NOX2–deficient cells, providing direct support that it was indeed gp91^{phox}/NOX2 being phosphorylated. In further support, p47^{phox} was phosphorylated normally in X°-CGD cells, which shows that PMA was able to induce protein phosphorylation in these cells and that the absence of the phospho-gp91^{phox}/NOX2 protein was due to the absence of gp91^{phox}/NOX2.

Deglycosylated gp91phox/NOX2 migrated as a sharper, more focused band at ~60 kDa, which is consistent with previous reports (42). Likewise, the phosphorylated broad band also shifted to a more focused 60 kDa band after deglycosylation of the protein isolated from ^{32}P-labeled cells. Together with our immunoprecipititation studies from normal and CGD neutrophils, these results clearly demonstrate that the phosphorylated protein immunoprecipitated here is indeed gp91^{phox}/NOX2.

Previously studies analyzed protein phosphorylation in cytochrome b_{558}-deficient neutrophils from CGD patients and suggested that gp91^{phox} and p22^{phox} were phosphorylated (45). Subsequently, phosphorylation of p22^{phox} has been confirmed and characterized (26);

however, the putative phosphorylation of gp91^{phox} has not been directly evaluated, nor have the pathways involved in this process been defined. One possible reason for this delay may have been the lack of specific immunoprecipitating antibodies. In this study, we used a specific monoclonal antibody that effectively immunoprecipitates gp91^{phox} to show that it is phosphorylated in stimulated human neutrophils. In addition, we confirmed these results by coimmunoprecipitating gp91^{phox} with a specific monoclonal antibody against p22^{phox}, because gp91^{phox} is always expressed as a heterodimer with p22^{phox}. In both cases phosphorylated gp91^{phox} was detected, which confirmed that gp91^{phox} is phosphorylated in activated human neutrophils. Likewise, phosphorylated p22^{phox} and phosphorylated p47^{phox} were also present in gp91^{phox}/NOX2 immunoprecipitates obtained with both antibodies (data not shown). Although the presence of phosphorylated p22^{phox} in activated neutrophils confirms previous studies (26), these are the first studies to demonstrate a clear phosphorylation of gp91^{phox}/NOX2.

Treatment of neutrophils with a range of neutrophil agonists significantly increased gp91^{phox}/NOX2 phosphorylation. The order of potency of these activators (PMA>OPZ>fMLP) generally corresponds to the activating potency of these agents for activation of the NADPH oxidase. PMA, a direct PKC activator, was the strongest inducer of gp91^{phox}/NOX2 phosphorylation, and GF109203X, a selective PKC inhibitor, strongly inhibited gp91^{phox}/NOX2 phosphorylation induced by PMA, as well as fMLP (data not shown). Although human neutrophils express many different PKC isoforms (α, β, δ, and ζ; refs. 41, 46), PMA primarily activates conventional isoforms (α and β). Because GF109203X also inhibits these specific isoforms, our studies suggested that α and β PKC isoforms participate in gp91^{phox}/NOX2 phosphorylation in human neutrophils, although the involvement of other PKC isoforms or other protein kinases is not excluded. To determine whether PKC directly phosphorylated gp91^{phox}/NOX2, we evaluated phosphorylation of a recombinant cytosolic region of gp91^{phox}/NOX2 by a mixture of α and β PKC isoforms and found that these isoforms were able to phosphorylate recombinant NOX2 (291-570) *in vitro* and that each PKC isoform (α, β, δ, and ζ) is able to phosphorylate gp91^{phox}/NOX2 (data not shown). Additionally, phosphoamino acid analysis of PKC-phosphorylated NOX2 (291-570) showed that this protein was phosphorylated on serine and threonine residues *in vitro,* which is characteristic of PKC activity.

Putative gp91^{phox}/NOX2 sequence organization suggests that, in addition to the cytosolic C-terminal sequence, it possesses a small N-terminal cytosolic tail (aa 1-9) and 2 cytosolic loops (aa 69-98 and 190-204) (10, 47). Both loops contain 2 PKC-consensus phosphorylation sequences (-R/KXS/T- or S/TXR/K-) (48, 49) and thus could also be phosphorylated by PKC. In comparison, the C-terminal cytosolic fragment contains up to 8 PKC-consensus phosphorylation sites, as detected by bioinformatics analysis. Two-dimensional tryptic phosphopeptide mapping analysis showed that PKC induced phosphorylation of the gp91^{phox}/NOX2 C-terminal domain *in vitro,* and phosphorylation was in the same locations as those phosphorylated in intact cells. Further localization of the phosphorylated residues was accomplished by CNBr cleavage. Results show that NOX2 is phosphorylated on the 13-kDa carboxy-terminal sequence (residues 466-570) and 10-kDa sequence (residues 321-405). These fragments contain 3 putative PKC phosphorylation sites: Ser-333, Thr509, and Ser-550.

The hydrophilic C-terminal domain of gp91^{phox}/NOX2 contains the FAD-binding and consensus NADPH-binding sequences (10, 14, 15), and it has been proposed that gp91^{phox}/NOX2 is the catalytic core of NADPH oxidase because it contains all the required factors (13–15). The NADPH oxidase appears to catalyze $O_2^{\cdot-}$ formation *via* a 2-step electron transfer process. The first step, catalyzed by the flavin center, is called diaphorase activity (16–19), and it has been shown previously that the cytosolic tail of gp91^{phox}/NOX2, which contains the flavoprotein domain, also exhibits NADPH diaphorase activity (18, 19). Currently little is known how this electron transfer process is induced and regulated. Here we show that phosphorylation of this region of gp91^{phox}/NOX2 induces an increase in diaphorase activity and binding to cytosolic proteins, which suggests the possibility that phosphorylation could induce a conformational change in the gp91^{phox}/NADPH, which may facilitate electron transfer or alignment/integration with other components of the chain, such as NADPH or FAD. Thus, it is possible that phosphorylation of the C-terminal cytosolic domain of gp91^{phox}/NOX2 may regulate its catalytic activity by facilitating step 1 of the activation cascade. In addition, NOX2 phosphorylation induced an increased binding to rac2, p67^{phox}, and p47^{phox}, and a further increase of diaphorase activity of the complex. Gp91^{phox}/NOX2 purified from neutrophils was shown to interact with the cytosolic components Rac2, p67^{phox}, and p47^{phox} (30). In this study we found that in the absence of phosphorylation the cytosolic fragment of NOX2 interacts with p67phox, p47phox, and Rac2 and the phosphorylation increased these interactions. Taken together, these results suggest that phosphorylation of gp91^{phox}/NOX2 may regulate the assembly of the complex and its catalytic activity in the absence and presence of cytosolic components.

Recently, several homologues of gp91^{phox}/NOX2 (NOX1 to NOX5) have been described in human tissues (lung, kidney, and colon) and in various cell types (epithelial cells, endothelial cells, vascular smooth muscle cells) (50, 51). Phosphorylation of NOX proteins can regulate their enzymatic activity, and Jagnandan *et al.* (52) recently showed that NOX5 is phosphorylated on Thr494 and Ser-498 in transfected COS7 cells and suggested that this phosphorylation facilitates NOX5 activation in the presence of low levels of intracellular calcium. To know whether the NOX5 phosphorylated sites are present in NOX2, we compared the 2 sequences, which reveals that the NOX5-sequences containing Thr494 and Ser-498 are absent in NOX2. This suggests that NOX2 and NOX5 are phosphorylated on different sites. Ogasawara *et al.* (53) also showed that the plant NOX2 homologue AtrbohD is phosphorylated and suggested that this phosphoryla-

tion and calcium binding synergistically activate this enzyme. Likewise, the results presented here support the idea that NOX electron transfer could be regulated by phosphorylation.

In conclusion, we showed that gp91^{phox}/NOX2 is phosphorylated in human neutrophils stimulated with a range of agonists, including PMA, fMLP, and OPZ. This phosphorylation seems to be mediated by PKC and enhances the interaction of gp91^{phox}/NOX2 with the cytosolic components and its diaphorase activity. Thus, our study suggests a novel mechanism by which NADPH oxidase activity could be regulated. Future studies are required to identify the specific phosphorylation sites and to evaluate the role of phosphorylation in regulating gp91^{phox}/NOX2 function in intact cells by site-directed mutagenesis. FJ

We dedicate this work to the memory of Bernard M. Babior, who is no longer among us. We thank Mary Dinauer (Herman B. Wells Center for Pediatric Research, Indiana University School of Medicine, Bloomington, IN, USA) and Ulla Knaus (Scripps Research Institute, La Jolla, CA, USA) for the generous gift of NOX2 cDNA and pGex-Rac2 plasmid. H. R. is a recipient of the FRM (Fondation pour la Recherche Médicale) fellowship. This work was supported by ARC (Association pour la Recherche sur le Cancer); the "Région Rhône-Alpes, program Emergence 2003," France; the CGD Research Trust 2006, UK; the "Délégation Régionale de la Recherche Clinique," CHU Grenoble, France; and U. S. National Institutes of Health grants AR42426 and RR020185.

REFERENCES

1. Segal, A. W. (2005) How neutrophils kill microbes. *Annu. Rev. Immunol.* **23,** 197–223
2. Dinauer, M. C. (1993) The respiratory burst oxidase and the molecular genetics of chronic granulomatous disease. *Crit. Rev. Clin. Lab. Sci.* **30,** 329–369
3. Chanock, S. J., El-Benna, J., Smith, R. M., and Babior, B. M. (1994) The respiratory burst oxidase. *J. Biol. Chem.* **269,** 24519–24522
4. Babior, B. M. (1984) Oxidants from phagocytes: agents of defense and destruction. *Blood* **64,** 959–966
5. Smith, J. A. (1994) Neutrophils, host defense, and inflammation: a double-edged sword. *J. Leukoc. Biol.* **56,** 672–686
6. El-Benna, J., Dang, P. M., Gougerot-Pocidalo, M. A., and Elbim, C. (2005) Phagocyte NADPH oxidase: a multicomponent enzyme essential for host defenses. *Arch. Immunol. Ther. Exp. (Wars.)* **53,** 199–206
7. Quinn, M. T., and Gauss, K. A. (2004) Structure and regulation of the neutrophil respiratory burst oxidase: comparison with nonphagocyte oxidases. *J. Leukoc. Biol.* **76,** 760–781
8. Groemping, Y., and Rittinger, K. (2005) Activation and assembly of the NADPH oxidase: a structural perspective. *Biochem. J.* **386,** 401–416
9. Babior, B. M. (1999) NADPH oxidase: an update. *Blood* **93,** 1464–1476
10. Vignais, P. V. (2002) The superoxide-generating NADPH oxidase: structural aspects and activation mechanism. *Cell. Mol. Life Sci.* **59,** 1428–1459
11. Yu, L., Zhen, L., and Dinauer, M. C. (1997) Biosynthesis of the phagocyte NADPH oxidase cytochrome b558: role of heme incorporation and heterodimer formation in maturation and stability of gp91phox and p22phox subunits. *J. Biol. Chem.* **272,** 27288–27294
12. DeLeo, F. R., Burritt, J. B., Yu, L., Jesaitis, A. J., Dinauer, M. C., and Nauseef, W. M. (2000) Processing and maturation of flavocytochrome b558 include incorporation of heme as a prerequisite for heterodimer assembly. *J. Biol. Chem.* **275,** 13986–13993
13. Koshkin, V., and Pick, E. (1993) Generation of superoxide by purified and relipidated cytochrome b559 in the absence of cytosolic activators. *FEBS Lett.* **327,** 57–62
14. Yu, L., Quinn, M. T., Cross, A. R., and Dinauer, M. C. (1998) Gp91(phox) is the heme binding subunit of the superoxide-generating NADPH oxidase. *Proc. Natl. Acad. Sci. U. S. A.* **95,** 7993–7998
15. Rotrosen, D., Yeung, C. L., Leto, T. L., Malech, H. L.,and Kwong, C. H. (1992) Cytochrome b558: the flavin-binding component of the phagocyte NADPH oxidase. *Science* **256,** 1459–1462
16. Li, J., and Guillory, R. J. (1997) Purified leukocyte cytochrome b558 incorporated into liposomes catalyzes a cytosolic factor dependent diaphorase activity. *Biochemistry* **36,** 5529–5537
17. Cross, A. R., Yarchover, J. L., and Curnutte, J. T. (1994) The superoxide-generating system of human neutrophils possesses a novel diaphorase activity: evidence for distinct regulation of electron flow within NADPH oxidase by p67-phox and p47-phox. *J. Biol. Chem.* **269,** 21448–21454
18. Han, C. H., Nisimoto, Y., Lee, S. H., Kim, E. T., and Lambeth, J. D. (2001) Characterization of the flavoprotein domain of gp91phox which has NADPH diaphorase activity. *J. Biochem.* **129,** 513–520
19. Nisimoto, Y., Ogawa, H., Miyano, K., and Tamura, M. (2004) Activation of the flavoprotein domain of gp91phox upon interaction with N-terminal p67phox (1–210) and the Rac complex. *Biochemistry* **43,** 9567–9575
20. Gérard, B., El Benna, J., Alcain, F., Gougerot-Pocidalo, M. A., Grandchamp, B., and Chollet-Martin, S. (2001) Characterization of 11 novel mutations in the X-linked chronic granulomatous disease (CYBB gene). *Hum. Mutat.* **18,** 163–166
21. El Benna, J., Faust, L. P., and Babior, B. M. (1994) The phosphorylation of the respiratory burst oxidase component p47phox during neutrophil activation: phosphorylation of sites recognized by protein kinase C and by proline-directed kinases. *J. Biol. Chem.* **269,** 23431–23436
22. Faust, L. P., El Benna, J., Babior, B. M., and Chanock, S. J. (1995) The phosphorylation targets of p47phox, a subunit of the respiratory burst oxidase: functions of the individual target serines as evaluated by site-directed mutagenesis. *J. Clin. Invest.* **96,** 1499–1505
23. El Benna, J., Faust, L. P., Johnson, J. L., and Babior, B. M. (1996) Phosphorylation of the respiratory burst oxidase subunit p47phox as determined by two-dimensional phosphopeptide mapping: phosphorylation by protein kinase C, protein kinase A, and a mitogen-activated protein kinase. *J. Biol. Chem.* **271,** 6374–6378
24. El-Benna, J., Dang, P. M. C., Gaudry, M,. Fay, M., Morel, F., Hakim, J., and Gougerot-Pocidalo, M. A. (1997) Phosphorylation of the respiratory burst oxidase subunit p67(phox) during human neutrophil activation: regulation by protein kinase C-dependent and independent pathways. *J. Biol. Chem.* **272,** 17204–17208
25. Bouin, A. P., Grandvaux, N., Vignais, P. V., and Fuchs, A. (1998) p40(phox) is phosphorylated on threonine 154 and serine 315 during activation of the phagocyte NADPH oxidase: implication of a protein kinase c-type kinase in the phosphorylation process. *J. Biol. Chem.* **273,** 30097–30103
26. Regier, D. S., Greene, D. G., Sergeant, S., Jesaitis, A. J., and McPhail, L. C. (2000) Phosphorylation of p22phox is mediated by phospholipase D-dependent and -independent mechanisms: correlation of NADPH oxidase activity and p22phox phosphorylation. *J. Biol. Chem.* **275,** 28406–288412
27. Heyworth, P. G., Curnutte, J. T., Nauseef, W. M., Volpp, B. D., Pearson, D. W., Rosen, H., and Clark, R. A. (1991) Neutrophil nicotinamide adenine dinucleotide phosphate oxidase assembly: translocation of p47-phox and p67-phox requires interaction between p47-phox and cytochrome b558. *J. Clin. Invest.* **87,** 352–356
28. Quinn, M. T., Evans, T., Loetterle, L. R., Jesaitis, A. J., and Bokoch, G. M. (1993) Translocation of Rac correlates with NADPH oxidase activation: evidence for equimolar translocation of oxidase components. *J. Biol. Chem.* **268,** 20983–20987
29. El Benna, J., Ruedi, J. M., and Babior, B. M. (1994) Cytosolic guanine nucleotide-binding protein Rac2 operates in vivo as

a component of the neutrophil respiratory burst oxidase: transfer of Rac2 and the cytosolic oxidase components p47phox and p67phox to the submembranous actin cytoskeleton during oxidase activation. *J. Biol. Chem.* **269,** 6729–6734
30. Dang, P. M., Cross, A. R., and Babior, B. M. (2001) Assembly of the neutrophil respiratory burst oxidase: a direct interaction between p67PHOX and cytochrome b558. *Proc. Natl. Acad. Sci. U. S. A.* **98,** 3001–3005
31. Burritt, J. B., Quinn, M. T., Jutila, Bond, C. W., and Jesaitis, A. J. (1995) Topological mapping of neutrophil cytochrome b epitopes with phage-display libraries. *J. Biol. Chem.* **270,** 16974–16980
32. Batot, G., Martel, C., Capdeville, N., Wientjes, F., and Morel, F. (1995) Characterization of neutrophil NADPH oxidase activity reconstituted in a cell-free assay using specific monoclonal antibodies raised against cytochrome b558. *Eur. J. Biochem.* **234,** 208–215
33. Dang, M. P., Dewas, C., Gaudry, M., Fay, M., Gougerot-Pocidalo, and El Benna, J. (1999) Priming of human neutrophil respiratory burst by granulocyte/macrophage colony-stimulating factor (GM-CSF) involves partial phosphorylation of p47(phox). *J. Biol. Chem.* **274,** 20704–20708
34. Dewas, C., Dang, P. M., Gougerot-Pocidalo, M. A., and El-Benna, J. (2003) TNF-alpha induces phosphorylation of p47(phox) in human neutrophils: partial phosphorylation of p47phox is a common event of priming of human neutrophils by TNF-alpha and granulocyte-macrophage colony-stimulating factor. *J. Immunol.* **171,** 4392–4398
35. Taylor, R. M., Burritt, J. B., Foubert, T. R., Snodgrass, M. A., Stone, K. C., Baniulis, D., Gripentrog, J. M., Lord, C., and Jesaitis, A. J. (2003) Single-step immunoaffinity purification and characterization of dodecylmaltoside-solubilized human neutrophil flavocytochrome b. *Biochim. Biophys. Acta* **1612,** 65–75
36. Batot, G., Paclet, M. H., Doussiere, J., Vergnaud, S., Martel, C., Vignais, P. V., and Morel, F. (1998) Biochemical and immunochemical properties of B lymphocyte cytochrome b558. *Biochim. Biophys. Acta* **1406,** 188–202
37. Laemmli, U. K. (1970) Cleavage of structural proteins during the assembly of the head of bacteriophage T4. *Nature* **227,** 680–685
38. Paclet, M. H., Henderson, L. M., Campion, Y., Morel, F., and Dagher, M. C. (2004) Localization of Nox2 N-terminus using polyclonal antipeptide antibodies. *Biochem. J.* **382,** 981–986
39. Dang, P. M., Stensballe, A., Boussetta, T., Raad, H., Dewas, C., Kroviarski, Y., Hayem, G., Jensen, O. N., Gougerot-Pocidalo, M. A., and El-Benna, J. (2006) A specific p47phox -serine phosphorylated by convergent MAPKs mediates neutrophil NADPH oxidase priming at inflammatory sites. *J. Clin. Invest.* **116,** 2033–2043
40. Zhen, L., King, A. A., Xiao, Y., Chanock, S. J., Orkin, S. H., and Dinauer, M. C. (1993) Gene targeting of X chromosome-linked chronic granulomatous disease locus in a human myeloid leukemia cell line and rescue by expression of recombinant gp91phox. *Proc. Natl. Acad. Sci. U. S. A.* **90,** 9832–9836
41. Fontayne, A., Dang, P. M., Gougerot-Pocidalo, M. A., and El-Benna, J. (2002) Phosphorylation of p47phox sites by PKC alpha, beta II, delta, and zeta: effect on binding to p22phox and on NADPH oxidase activation. *Biochemistry* **41,** 7743–7750
42. Paclet, M. H., Coleman, A. W., Burritt, J., and Morel, F. (2001) NADPH oxidase of Epstein-Barr-virus immortalized B lymphocytes: effect of cytochrome b(558) glycosylation. *Eur. J. Biochem.* **268,** 5197–5208
43. Wallach, T. M., and Segal, A. W. (1997) Analysis of glycosylation sites on gp91phox, the flavocytochrome of the NADPH oxidase, by site-directed mutagenesis and translation in vitro. *Biochem. J.* **321,** 583–585
44. Kao, Y. Y., Gianni, D., Bohl, B., Taylor, R. M., and Bokoch, G. M. (2008) Identification of a conserved Rac-binding site on NADPH oxidases supports a direct GTPase regulatory mechanism. *J. Biol. Chem.* **283,** 12736–12746
45. Garcia, R. C., and Segal, A. W. (1988) Phosphorylation of the subunits of cytochrome b-245 upon triggering of the respiratory burst of human neutrophils and macrophages. *Biochem. J.* **252,** 901–904
46. Dang, P. M., Fontayne, A., Hakim, J., El Benna, J., and Perianin, A. (2001) Protein kinase C zeta phosphorylates a subset of selective sites of the NADPH oxidase component p47phox and participates in formyl peptide-mediated neutrophil respiratory burst. *J. Immunol.* **166,** 1206–1213
47. Burritt, J. B., Foubert, T. R., Baniulis, D., Lord, C. I., Taylor, R. M., Mills, J. S., Baughan, T. D., Roos, D., Parkos, C. A., and Jesaitis, A. J. (2003) Functional epitope on human neutrophil flavocytochrome b558. *J. Immunol.* **170,** 6082–6089
48. Kennelly, P. J., and Krebs, E. G. (1991) Consensus sequences as substrate specificity determinants for protein kinases and protein phosphatases. *J. Biol. Chem.* **266,** 15555–15558
49. Hofmann, J. (1997) The potential for isoenzyme-selective modulation of protein kinase C. *FASEB J.* **11,** 649–669
50. Lambeth, J. D. (2004) NOX enzymes and the biology of reactive oxygen. *Nat. Rev. Immunol.* **4,** 181–189
51. Bedard, K., and Krause, K. H. (2007) The NOX family of ROS-generating NADPH oxidases: physiology and pathophysiology. *Physiol. Rev.* **87,** 245–313
52. Jagnandan, D., Church, J. E., Banfi, B., Stuehr, D. J., Marrero, M. B., and Fulton, D. J. (2007) Novel mechanism of activation of NADPH oxidase 5: calcium sensitization via phosphorylation. *J. Biol. Chem.* **282,** 6494–6507
53. Ogasawara, Y., Kaya, H., Hiraoka, G., Yumoto, F., Kimura, S., Kadota, Y., Hishinuma, H., Senzaki, E., Yamagoe, S., Nagata, K., Nara, M., Suzuki, K., Tanokura, M., and Kuchitsu, K. (2008) Synergistic activation of the Arabidopsis NADPH oxidase AtrbohD by Ca2+ and phosphorylation. *J. Biol. Chem.* **283,** 8885–8892

Received for publication June 3, 2008.
Accepted for publication October 30, 2008.